

## MODELING OF PHASE DIAGRAM OF THE SYSTEM $\text{BiI}_3\text{-Bi}_2\text{S}_3\text{-Bi}_2\text{Te}_3$

E.J. Ahmadov<sup>1\*</sup>, A.N. Mammadov<sup>1,2</sup>, S.A. Guliyeva<sup>3</sup>, M.B. Babanly<sup>1</sup>

<sup>1</sup>Institute of Catalysis and Inorganic Chemistry, Azerbaijan National Academy of Science, Baku, Azerbaijan

<sup>2</sup>Azerbaijan Technical University, Baku, Azerbaijan

<sup>3</sup>Azerbaijan State Pedagogical University, Baku, Azerbaijan

**Abstract.** Using the 2D and 3D option of the computer Origin Lab, analytical dependencies of the liquidus temperatures on the composition for the binary and three-component phases of the system  $\text{BiI}_3\text{-Bi}_2\text{S}_3\text{-Bi}_2\text{Te}_3$  were obtained, which allowed to visualize the crystallization surfaces of the  $\text{Bi}_2\text{S}_3$ ,  $\text{Bi}_2\text{Te}_3$ ,  $\text{BiSI}$ ,  $\text{Bi}_{19}\text{S}_{27}\text{I}_3$ ,  $\text{BiTeI}$  and  $\text{Bi}_2\text{Te}_2\text{S}$  separately and of all phases of the system  $\text{BiI}_3\text{-Bi}_2\text{S}_3\text{-Bi}_2\text{Te}_3$  on one graph.

**Keywords:**  $\text{BiI}_3\text{-Bi}_2\text{S}_3\text{-Bi}_2\text{Te}_3$  system, 3D analytical modeling, liquidus surfaces.

**Corresponding Author:** Elvin Ahmadov, Institute of Catalysis and Inorganic Chemistry named after acad. M. Nagiyev, Azerbaijan National Academy of Sciences, 113, H. Javid. ave., AZ-1143, Baku, Azerbaijan, Tel: +994 50 537 51 07, e-mail: [elvin.ahmedov.2014@mail.ru](mailto:elvin.ahmedov.2014@mail.ru)

**Received:** 14 March 2021;

**Accepted:** 25 April 2021;

**Published:** 30 April 2021.

### 1. Introduction

Chalcohalides of arsenic subgroup elements, in particular, bismuth chalcogenides have been the focus of attention of researchers as valuable ferroelectric, thermoelectric, photovoltaic, magnetic, and optical materials (Koc *et al.*, 2017; Hahn *et al.*, 2012; Khan *et al.*, 2017; Ganose *et al.*, 2016). In the last few years, it has been determined that bismuth tellurohalides and phases on their basis also show the properties of a topological insulator and demonstrate 3D Rashba spin splitting, which opens up the possibilities to use them in spintronic devices (Ishizaka *et al.*, 2011; Landolt *et al.*, 2012; Ereemeev *et al.*, 2017; Li *et al.*, 2020; Wu *et al.*, 2016; Maa *et al.*, 2016; Gennep *et al.*, 2014). The phase equilibria in  $\text{Bi-S(Te)-I}$  systems were studied, the projection of liquidus surfaces was constructed, melting character and primary crystallization regions of existing phases were determined (Aliiev *et al.*, 2014; Babanly *et al.*, 2009). In Ahmadov, (2020) based on the results of the DTA and X-ray diffraction analysis, the phase equilibria in the  $\text{BiTeI-BiSI}$  system were studied and the  $T-x$  phase diagram was constructed. It was established that the system is stable in the subsolidus area and there are ~7–8 mol % and ~5 mol% solid solution areas based on  $\text{BiTeI}$  and  $\text{BiSI}$  compounds at room temperature, accordingly. The system is non-quasibinary.  $\text{Bi}_{19}\text{S}_{27}\text{I}_3$  (0–33 mol %  $\text{BiTeI}$ ) and tetradymite- $\text{Bi}_2\text{Te}_2\text{S}$  (33–83 mol%  $\text{BiTeI}$ ) phases primarily crystallize from the liquid phase in the wide composition ranges. In Ahmadov *et al.*, (2021) phase equilibria in the quasi-ternary system  $\text{Bi}_2\text{S}_3\text{-Bi}_2\text{Te}_3\text{-BiI}_3$  were studied by differential thermal analysis, powder X-ray diffraction analysis, and scanning electron microscopy. The isothermal sections at 300, 750, 800, and 850 K and some polythermal sections and a projection of the liquidus surface were constructed. The primary crystallization fields

and homogeneity regions of phases, and the types and coordinates of in- and monovariant equilibria were determined. It was shown that the system is characterized by the formation of limited regions of solid solutions based on bismuth sulfide and telluride, and also ternary compounds  $\text{Bi}_2\text{Te}_2\text{S}$ ,  $\text{BiSI}$ , and  $\text{BiTeI}$ .

However, to date the phase diagram of  $\text{BiI}_3\text{-Bi}_2\text{S}_3\text{-Bi}_2\text{Te}_3$  system is not modeled. The analytical model of the phase diagram, in particular the 3D model of the crystallization surface of the phases, is very useful for choosing the optimal conditions for obtaining solid phases by crystallization of liquid alloys of the  $\text{BiI}_3\text{-Bi}_2\text{S}_3\text{-Bi}_2\text{Te}_3$  system. The aim of this work is analytical 3D modeling of crystallization surfaces of all phases of the ternary system  $\text{BiI}_3\text{-Bi}_2\text{S}_3\text{-Bi}_2\text{Te}_3$  based on the data of boundary systems and a small number of experimental DTA measurements.

## 2. Modeling Technique

For 3D modeling of crystallization surfaces in the  $\text{BiI}_3\text{-Bi}_2\text{S}_3\text{-Bi}_2\text{Te}_3$  system, an analytical method was used, which was previously successfully tested in Yusibov et al., (2017, 2018). With regard to the three-component  $\text{BiI}_3\text{-Bi}_2\text{S}_3\text{-Bi}_2\text{Te}_3$  system, the temperature dependences of the crystallization surface are determined as a function

$$T = f(x, y) \quad (1)$$

where:  $x$  - is the relative mole fraction  $\text{Bi}_2\text{S}_3$ :  $y(\text{Bi}_2\text{S}_3)/[y(\text{Bi}_2\text{S}_3)+ y(\text{Bi}_2\text{S}_3)]$  and  $y$  - is mole fraction of  $\text{BiI}_3$  in ternary system  $\text{BiI}_3\text{-Bi}_2\text{S}_3\text{-Bi}_2\text{Te}_3$ .

The obtained analytical expressions for the ternary system the  $\text{BiI}_3\text{-Bi}_2\text{S}_3\text{-Bi}_2\text{Te}_3$  and its binary boundary systems are given in Tables 1 and 2. The analytical dependences are presented in the form used by the Origin Lab computer program.

Modeling is carried out in this order. First, the temperature dependences on the composition are determined  $T = f(x)$  and  $T = f(y)$  for the liquidus of binary boundary systems. Next, on the basis of using the experimental ternary the  $\text{BiI}_3\text{-Bi}_2\text{S}_3\text{-Bi}_2\text{Te}_3$  system defined function  $T = f(x, y)$ .

### 2.1. Binary boundary systems

The boundary quasi-binary constituents of the system  $\text{BiI}_3\text{-Bi}_2\text{S}_3\text{-Bi}_2\text{Te}_3$  have been studied in detail (Aliev *et al.*, 2014; Babanly *et al.*, 2009; Yusa *et al.*, 1979; Kuznetsov & Kanishcheva, 1970). In the system  $\text{Bi}_2\text{S}_3\text{-BiI}_3$  (Fig.1), two ternary compounds,  $\text{BiSI}$  and  $\text{Bi}_{19}\text{S}_{27}\text{I}_3$ , form, which melt with decomposition by peritectic reactions at 808 and 990 K, respectively (Aliev *et al.*, 2014). The compound  $\text{BiSI}$  crystallizes in the orthorhombic symmetry, and  $\text{Bi}_{19}\text{S}_{27}\text{I}_3$  has a hexagonal lattice. In the system  $\text{Bi}_2\text{Te}_3\text{-Bi}_2\text{S}_3$  (Yusa *et al.*, 1979; Kuznetsov & Kanishcheva, 1970), a variable-composition phase forms, the homogeneity region of which includes the mineral tetradymite  $\text{Bi}_2\text{Te}_2\text{S}$ . This compound melts congruently at 898 K and has a rhombohedral structure. The phase diagram of the system  $\text{Bi}_2\text{Te}_3\text{-BiI}_3$  is characterized by the formation of the ternary compound  $\text{BiTeI}$ , which congruently melts at 828 K (Babanly *et al.*, 2009) and has a trigonal structure.

The phase diagrams of the quasi-binary boundary systems  $\text{BiI}_3\text{-Bi}_2\text{S}_3$ ,  $\text{BiI}_3\text{-Bi}_2\text{Te}_3$  and  $\text{Bi}_2\text{S}_3\text{-Bi}_2\text{Te}_3$  and their analytical dependences for liquidus lines are shown in Table 1. Analytical dependencies are determined using the "analysis" option of the OriginLab computer program. From Fig. 1 it is shown that the obtained analytical dependence with

sufficient accuracy approximates the liquidus curve of compound  $\text{BiTeI}$  in the system  $\text{BiI}_3\text{-Bi}_2\text{Te}_3$ .

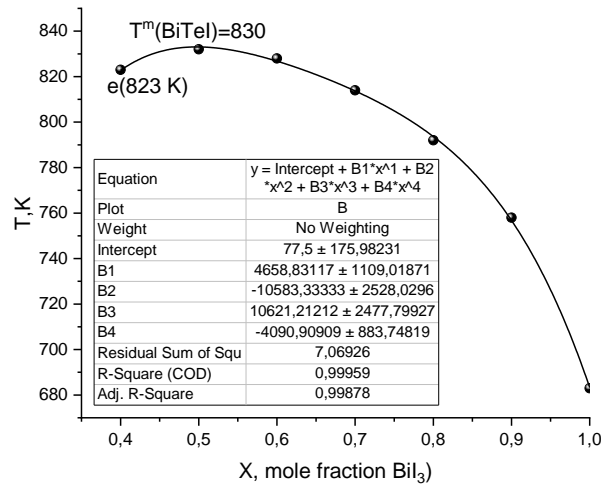
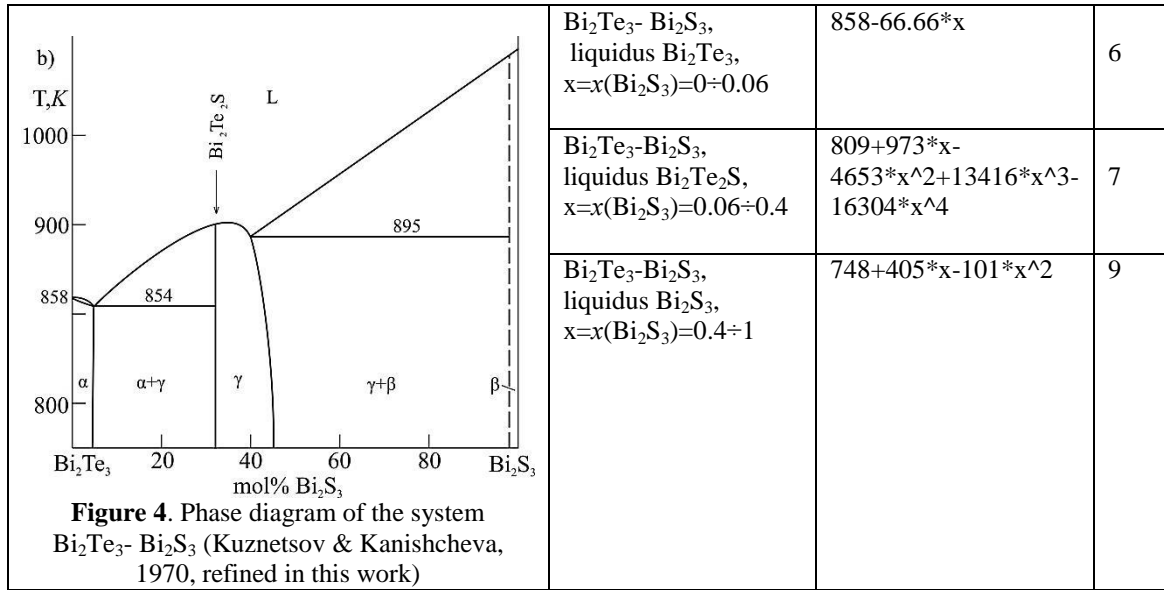


**Figure 1.** Dependence of the liquidus temperatures of the compound  $\text{BiTeI}$  on the composition in the system  $\text{BiI}_3\text{-Bi}_2\text{Te}_3$ : curve-polynomial, symbol-experiment (Babanly *et al.*, 2009).

**Table 1.** Phase diagrams and analytical dependencies for their liquidus line of the  $\text{BiI}_3\text{-Bi}_2\text{S}_3$ ,  $\text{BiI}_3\text{-Bi}_2\text{Te}_3$  and  $\text{Bi}_2\text{S}_3\text{-Bi}_2\text{Te}_3$  systems (equations are presented in computer variation)

Phase diagram	System, region	Equations: $T, K=f(x)$	Eq. N
	$\text{BiI}_3\text{-Bi}_2\text{S}_3$ , liquidus $\text{BiSI}$ , $x=x(\text{Bi}_2\text{S}_3)=0.045 \div 0.3$	$634+800*x-860*x^2$	1
	$\text{BiI}_3\text{-Bi}_2\text{S}_3$ , liquidus $\text{Bi}_{19}\text{S}_{27}\text{I}_3$ , $x=x(\text{Bi}_2\text{S}_3)=0.35 \div 0.8$	$498+1094*x-600*x^2$	2
	$\text{BiI}_3\text{-Bi}_2\text{S}_3$ , liquidus $\text{Bi}_2\text{S}_3$ , $x=x(\text{Bi}_2\text{S}_3)=0.8 \div 1.0$	$-58+2110*x-1000*x^2$	3
	$\text{BiI}_3\text{-Bi}_2\text{Te}_3$ , liquidus $\text{Bi}_2\text{Te}_3$ , $x=x(\text{BiI}_3)=$ $0 \div 0.4$	$858-42,7*x+$ $121,4*x^2-583*x^3$	4
	$\text{BiI}_3\text{-Bi}_2\text{Te}_3$ , liquidus $\text{BiTeI}$ , $x=x(\text{BiI}_3)=$ $0.4 \div 1$	$14+5095*x-$ $11667*x^2+11783*x^3$ $-4545*x^4$	5



## 2.2. System $\text{Bi}_2\text{I}_3$ - $\text{Bi}_2\text{S}_3$ - $\text{Bi}_2\text{Te}_3$

The analytical dependences for 3D modeling of the liquidus surfaces of the  $\text{Bi}_2\text{S}_3$ ,  $\text{Bi}_2\text{Te}_3$ ,  $\text{BiSI}$ ,  $\text{Bi}_{19}\text{S}_{27}\text{I}_3$ ,  $\text{BiTeI}$  and  $\text{Bi}_2\text{Te}_2\text{S}$  phases are given in Table 2 (equations 10-15). These equations allow visualizing the crystallization surfaces separately (Fig. 5) and on one graph of all phases (Fig. 6).

**Table 2.** Analytical dependencies for phase diagram of the  $\text{BiI}_3$ - $\text{Bi}_2\text{S}_3$ - $\text{Bi}_2\text{Te}_3$  system

Compound liquidus surface	$T, K=f(x, y)$ ; $x= y(\text{Bi}_2\text{S}_3/[y(\text{Bi}_2\text{S}_3)+ y(\text{Bi}_2\text{S}_3)]); y=y(\text{BiI}_3)$ ; $y_i$ =mole fractions $\text{BiI}_3, \text{Bi}_2\text{S}_3, \text{Bi}_2\text{Te}_3$	Eq.N.
$\text{BiSI}$	$(634+800*(1-y)-860*(1-y)^2)*x^{0.2}$ ; $x=0.4-1; y=0.6-0.945$	10
$\text{Bi}_{19}\text{S}_{27}\text{I}_3$	$(498+1094*(1-y)-600*(1-y)^2)*x^{0.18}$ ; $x=0.3-1; y=0.2-0.65$	11
$\text{Bi}_2\text{S}_3$	$(748+405*x-101*x^2)*(1-y)^{0.27}$ ; $x=0.4-1; y=0-0.2$	12
$\text{Bi}_2\text{Te}_3$	$(858-42,7*y+121,4*y^2-583*y^3)*(1-x)^{0.2}$ ; $x=0-0.2; y=0-0.4$	13
$\text{BiTeI}$	$(14+5095*y-11667*y^2+11783*y^3-4545*y^4)*(1-x)^{0.2}$ ; $x=0-0.3; y=0.4-1$	14
$\text{Bi}_2\text{Te}_2\text{S}$	$(809+973*x-4653*x^2+13416*x^3-16304*x^4)*(1-y)^{0.25}$ ; $x=0.13-0.5; y=0-0.8$	15

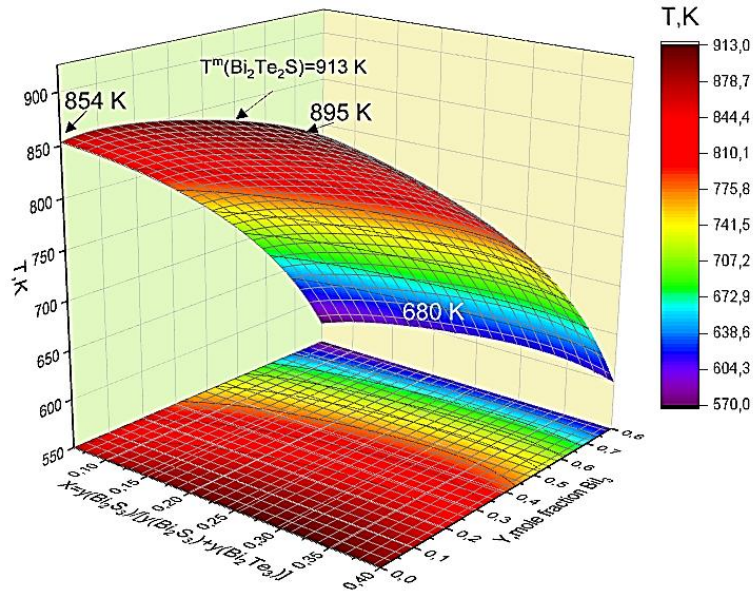


**Figure 5.** 3D model of crystallization surface  $\text{Bi}_2\text{Te}_2\text{S}$ , visualized by the equation 15 in table 2

The crystallization surfaces of all compounds in the  $\text{BiI}_3\text{-Bi}_2\text{S}_3\text{-Bi}_2\text{Te}_3$  system are visualized in Fig. 6, where the 3D dimensional phase diagram of the system is viewed from the side of the  $\text{BiI}_3\text{-Bi}_2\text{Te}_3$  system, from top to bottom.

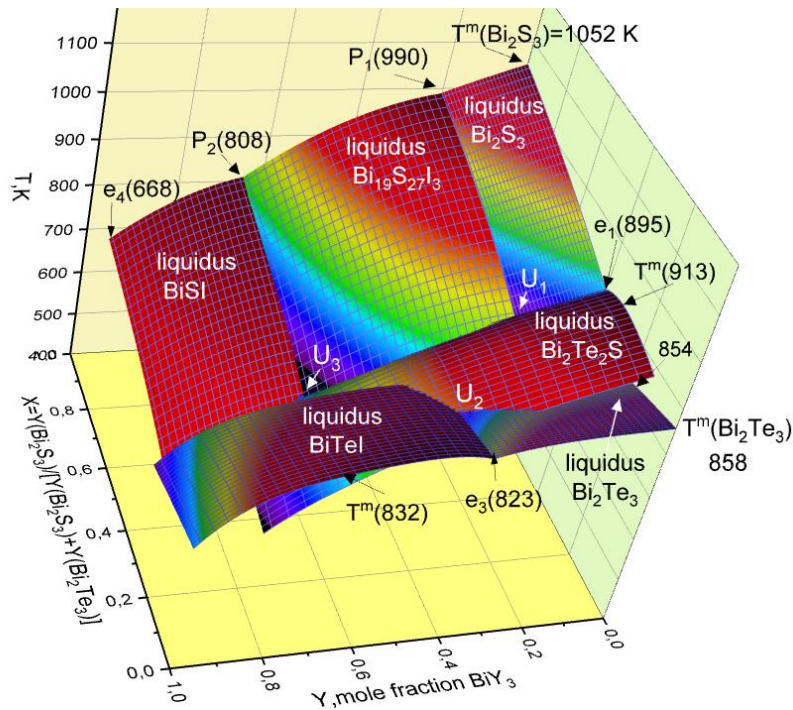


**Figure 6.** Multi-3D model of crystallization surfaces of the  $\text{Bi}_2\text{S}_3\text{-Bi}_2\text{Te}_3\text{-BiI}_3$  system, visualized by the equations 10-15 in table 2



### 3. Conclusion

The obtained analytical dependences of the liquidus temperatures on the composition made it possible to visualize the crystallization surfaces of the  $\text{Bi}_2\text{S}_3$ ,  $\text{Bi}_2\text{Te}_3$ ,  $\text{BiSI}$ ,  $\text{Bi}_{19}\text{S}_{27}\text{I}_3$ ,  $\text{BiTeI}$  and  $\text{Bi}_2\text{Te}_2\text{S}$  separately and of all phases of the  $\text{BiI}_3$ - $\text{Bi}_2\text{S}_3$ - $\text{Bi}_2\text{Te}_3$  system on one graph. Analytical dependences obtained using 2D and 3D option of the OriginLab program.  $100 \times 100 = 10,000$  and  $50 \times 50 = 2500$  tabular data in the form of matrices that can be used when choosing the optimal values of the composition, temperature for synthesis of binary and three-component phases  $\text{BiI}_3$ - $\text{Bi}_2\text{S}_3$ - $\text{Bi}_2\text{Te}_3$  systems.

### References

- Ahmadov, E.J. (2020). Physico-chemical interaction in the  $\text{BiSI}$ - $\text{BiTeI}$  system. *Azerb. Chem. J.*, 1, 35-40.
- Ahmadov, E.J., Aliev, Z.S., Babanly, D.M., Imamaliyeva, S.Z., Gasymov, V.A., Babanly, M.B. (2021). The Quasi-Ternary System  $\text{Bi}_2\text{S}_3$ - $\text{Bi}_2\text{Te}_3$ - $\text{BiI}_3$ . *Russ. J. Inorg. Chem.*, 66(4), 538-549.
- Aliev, Z.S., Musaeva, S.S., Jafarli, F.Y., Amiraslanov, I.R., Shevelkov, A.V., Babanly, M.B. (2014). The phase equilibria in the  $\text{Bi-S-I}$  ternary system and thermodynamic properties of the  $\text{BiSI}$  and  $\text{Bi}_{19}\text{S}_{27}\text{I}_3$  ternary compounds. *J. Alloys Compd.*, 610, 522-528.
- Babanly, M.B., Tedenac, J.C., Aliev, Z.S., Balitsky, D.M. (2009). Phase equilibria and thermodynamic properties of the system  $\text{Bi-Te-I}$ . *J. Alloys Compd.*, 481(1-2), 349-353.
- Eremeev, S.V., Nechaev, I.A., Chulkov, E.V. (2017). Two- and three-dimensional topological phases in  $\text{BiTeX}$  compounds. *Phys. Rev. B.*, 96(15), 1-9.
- Ganose, A.M., Butler, K.T., Walsh, A., Scanlon, D.O. (2016). Relativistic electronic structure and band alignment of  $\text{BiSI}$  and  $\text{BiSeI}$ : candidate photovoltaic materials. *J. Mater. Chem. A.*, 4(6), 2060-2068.
- Gennep, D.V., Maiti, S., Graf, D., Tozer, S.W., Martin, C., Berger, H., Maslov, D.L., Hamlin, J.J. (2014). Pressure tuning the Fermi level through the Dirac point of giant Rashba semiconductor  $\text{BiTeI}$ . *J. Phys.: Condens. Matter.*, 26(34), 342202-342208.
- Hahn, N.T., Rettie, A.J.E., Beal, S.K., Fullon, R.R., Mullins, C.B. (2012). n- $\text{BiSI}$  Thin films: selenium doping and solar cell behavior. *J. Phys. Chem. C.*, 116, 24878-24886.
- Ishizaka, K., Bahramy, M.S., Murakawa, H., Sakano, M., Shimojima, T., Sonobe, T., Koizumi, K., Shin, S., Miyahara, H., Kimura, A., Miyamoto, K., Okuda, T., Namatame, H., Taniguchi, M., Arita, R., Nagaosa, N., Kobayashi, K., Murakami, Y., Kumai, R., Kaneko, Y., Onose, Y., Tokura, Y. (2011). Giant Rashba-type spin splitting in bulk  $\text{BiTeI}$ . *Nat. Mater.*, 10(7), 521-526.
- Khan, W., Hussain, S., Minar, J., Azam, S. (2017). Electronic and Thermoelectric Properties of Ternary Chalcogenide Semiconductors: First Principles Study. *J. Elec. Materials*, 47(2), 1131-1139.
- Koc, H., Palaz, S., Mamedov, A.M., Ozbay, E. (2017). Optical, electronic, and elastic properties of some  $\text{A}^3\text{B}^6\text{C}^7$  ferroelectrics ( $\text{A}=\text{Sb, Bi}$ ;  $\text{B}=\text{Te, S, Se}$ ;  $\text{C}=\text{I, Br, Cl}$ ): First principle calculation. *Ferroelectrics*, 511, 22-34.
- Kuznetsov, V.G., Kanishcheva, A.S. (1970). X-ray study of alloys of the  $\text{Bi}_2\text{Te}_3$ - $\text{Bi}_2\text{S}_3$  system. *Neorg. Mater.*, 6, 1268-1271.
- Landolt, G., Eremeev, S.V., Koroteev, Y.M., Slomski, B., Muff, S., Neupert, T., Kobayashi, M., Strocov, V.N., Schmitt, T., Aliev, Z.S., Babanly, M.B., Amiraslanov, I.R., Chulkov, E.V., Osterwalder, J., Dil, J.H. (2012). Disentanglement of Surface and Bulk Rashba Spin Splittings in Noncentrosymmetric  $\text{BiTeI}$ . *Rew. Phys. Rev. Letters.*, 109(11), 1-5.

- Li, X., Sheng, Y., Wu, L., Hu, S., Yang, J., Singh, D.J., Yang, J., Zhang, W. (2020). Defect-mediated Rashba engineering for optimizing electrical transport in thermoelectric BiTeI. *Npj. Comput. Mater.*, 6(1), 107-113.
- Maa, H., Bentmann, H., Seibel, C., Tusche, C., Eremeev, S.V., Peixoto, T.R.F., Tereshchenko, O.E., Kokh, K.A., Chulkov, E.V., Kirschner, J., Reinert, F. (2016). Spin-texture inversion in the giant Rashba semiconductor BiTeI. *Nat. Commun.*, 7, 11621-11627.
- Wu, L., Yang, J., Zhang, T., Wang, S., Wei, P., Zhang, W., Chen, L., Yang, J. (2016). Enhanced thermoelectric performance in the Rashba semiconductor BiTeI through band gap engineering. *J. Phys.: Condens. Matter.*, 28(8), 085801-085807.
- Yusa, K., Sugaki, A., Kitakaze, A. Phase relation of some sulfide systems. (1979). *J. Jpn. Assoc. Min.*, 74, 162.
- Yusibov, Yu.A., Alverdiev, I.Dzh., Ibragimova, F.S., Mamedov, A.N., Tagiev, D.B., Babanly, M.B. (2017). Study and 3D Modeling of the Phase Diagram of the Ag-Ge-Se System. *Rus. J. Inorg. Chem.*, 62(9), 1223-1233.
- Yusibov, Yu, A., Alverdiev, I.Dzh., Mashadieva, L.F., Babanly, D.M., Mamedov, A.N., Babanly, M.B. (2018). Experimental Study and 3D Modeling of the Phase Diagram of the Ag-Sn-Se System. *Russ. J. Inorg. Chem.*, 63(12), 1622-1635.